

Diffusion in mixed A - B alloys in two and three dimensions

Nagwa El-Meshad and R. A. Tahir-Kheli

Department of Physics, Temple University, Philadelphia, Pennsylvania 19122

(Received 21 January 1985)

Precision Monte Carlo simulations of labeled particle diffusion in mixed A - B alloys in two and three dimensions are reported. A variety of concentrations and ratios of the hopping rates $J^B/J^A = \eta$ are analyzed. Results are compared with those predicted by available theories. The validity of these theories is observed to be strictly limited to the region where $\eta > 1/z$ (z is the lattice coordination number).

I. INTRODUCTION

In the preceding paper¹ (henceforth to be referred to as I), a detailed account of tracer diffusion in two-dimensional isotropic and anisotropic lattices was given. That presentation included an improved theory as well as a variety of accurate, large effective grand-sample (GS) precision simulations. One of the tidy features of that work was the excellent correspondence between the theory and the simulations.

Unfortunately, such a successful agreement cannot be achieved for the mixed alloy system consisting of macroscopic concentrations of at least two varieties of atoms. In this regard the fault, of course, lies with the theory. The Monte Carlo simulations for the mixed system present no essential difficulty.

In Sec. II, a brief review of the current status of the various theories is given. The simulations in two dimensions are described and the analyses of the data are discussed in Sec. III. The results for two dimensions are presented next in Sec. IV. Sections V and VI deal with the three-dimensional systems. A discussion of the results and some final remarks are included in Sec. VII.

II. BRIEF REVIEW OF THE THEORY

Manning² appears to have been the first to seriously address the problem of tracer diffusion in a mixed, multicomponent alloy. His analysis dealt with an important limiting situation where the vacancy concentration v is vanishingly small. Accordingly, if the constituent atom concentration for the species λ is c^λ , his work applies to the limit

$$v = \left[1 - \sum_{\lambda} c^{\lambda} \right] \rightarrow 0. \quad (2.1)$$

One of the traditional approaches to discussions of the tracer diffusion correlation factor f^0 , in single-component alloys with vanishing vacancy concentration is to write³

$$f^0 = H / (H + 2J^0) \quad \text{for } v = 0. \quad (2.2)$$

Here, J^0 is the hopping rate of the unique tracer and

$$H = JM, \quad (2.3a)$$

$$M = -(1 + \langle \cos\theta \rangle) / \langle \cos\theta \rangle. \quad (2.3b)$$

The background particles have hopping rate J and $\langle \cos\theta \rangle$ is the well-known geometrical parameter of the lattice used in I.

For the multicomponent alloy, Manning's work² amounts to introducing an ansatz for an effective single hopping parameter J^{eff} :

$$J^{\text{eff}} = \sum_{\lambda} \left[J^{\lambda} c^{\lambda} f^{\lambda} / \sum_{\lambda} J^{\lambda} c^{\lambda} \right]. \quad (2.4)$$

To make the analysis self-consistent, Eqs. (2.2) and (2.3) are rewritten in an "effective" form, i.e.,

$$f^0 = H^{\text{eff}} / (H^{\text{eff}} + 2J^0), \quad (2.5a)$$

where

$$H^{\text{eff}} = MJ^{\text{eff}}. \quad (2.5b)$$

For an n -component alloy, Eqs. (2.5a) and (2.5b) constitute a set of $n+1$ coupled equations in $n+1$ unknowns f^0 and f^{λ} . [Note, in this context Eq. (2.5a) can be rewritten a total of n additional times by designating the tracer as one of the background atoms of, say, species λ whereby, in Eq. (2.5a), $f^0 \rightarrow f^{\lambda}$ and $J^0 \rightarrow J^{\lambda}$. Similarly, if the tracer happens to be identical to one of the n varieties of atoms in the background, the set of equations (2.5a) and (2.5b) has only n distinct members.]

Although seemingly different, the viewpoint expressed above⁴ is in substance entirely equivalent to that of Manning.² Moreover, it has the advantage that it identifies the essence of the Manning ansatz in a form that lends itself to useful further generalization.^{5,6}

Manning's predictions were first tested in a detailed set of Monte Carlo simulations on bcc and fcc lattices by DeBruin *et al.*,⁴ who arrived at two important conclusions. First, they declared that "The agreement between results by the simulation method and from Manning's calculations is excellent if the vacancy-atom exchange rates for the (two) components do not differ by much more than one order of magnitude." Second, they stated that "The Kikuchi-Sato model (Ref. 7), which was developed for *ordered* alloys, is not very successful for calculating correlation factors in *random* alloys. This is shown clearly by the considerable deviations over the entire frequency range and the incorrect values for self-diffusion correlation factors."

In the present context, the above remarks may be interpreted as follows: For a two-component alloy consisting of *A* and *B* atoms, Manning's theory is reliable as long as the hopping rates are within the limits

$$J^B/J^A = \eta > 1/z. \quad (2.6)$$

Here, J^A and J^B are the hopping rates of the fast and the slow atoms, respectively. [Note, any more precise conclusions than this ought not to be drawn from the simulations reported in Ref. 4 where the sample sizes were in general relatively small (i.e., between $5 \times 5 \times 5$ and $19 \times 19 \times 19$) and the effective grand-sample sizes were not quite large enough (total *vacancy jumps* analyzed were approximately half a million).]

Similar conclusions can again be drawn from a later Monte Carlo work on a simple-cubic lattice by three of the same authors.⁸ Here the effective sample sizes were similar and the lattice sizes were $13 \times 13 \times 13$ and $19 \times 19 \times 19$.

The Manning theory is thus seen to be relatively successful in three dimensions. Even though in Refs. 4 and 8 only three-dimensional systems were analyzed, in view of the fact that diffusion in two dimensions is not too different (note, however, the small logarithmic corrections), the substance of the above remarks can be expected to apply also to two dimensions.

Despite this success, Manning's theory suffers from an important limitation in that its applicability is restricted to the case of vanishing vacancy concentration. In view of the rapid changes in the dynamic characteristics of a tracer near the $v \rightarrow 0$ threshold,⁹ the $v \rightarrow 0$ theory cannot safely be applied even to the relatively small vacancy concentration limit of $v \sim \frac{1}{10}$. (This contrasts strongly with the $1 - v = c \rightarrow 0$ limit results, which can often be applied, after simple mean-field-like corrections, to the cases $c < 0.25$.)

An attempt to extend the Manning theory to finite vacancy concentration has been made by Tahir-Kheli.⁵ In this work, the representation of Manning's final expressions in the form given in Eqs. (2.4)–(2.5b) is exploited by analogy with the single-component $v \rightarrow 0$ work³ and its finite vacancy concentration extension achieved by Tahir-Kheli and Elliot⁹ (henceforth to be referred to as TKE). The net result is that H^{eff} is transformed from its original form (2.5b) into the following:

$$H^{\text{eff}} = [M/(1-v)](vJ^0 f^0 + J^{\text{eff}}). \quad (2.7)$$

Clearly, for $v \rightarrow 0$, Eq. (2.6) reduces to Manning's result (2.5b). Similarly, for arbitrary v , but for a single-component background, Eqs. (2.5a) and (2.6) together reduce to the TKE result [see Eq. (3.19) of Ref. 9].

Motivated as it is from the small-vacancy end, at the opposite-concentration end, i.e., for small-particle concentrations (where $c^\lambda \ll 1$ for any λ and $\sum_\lambda c^\lambda = c \ll 1$), the above self-consistent theory is incorrect in the leading order c^λ (of course, it is exact when $c = 0$). On the other hand, for the intermediate concentrations, it can be expected to be moderately accurate for the diffusion correlation factor, especially that referring to the slow atoms. However, outside the range (2.6), this theory cannot be expected to provide accurate results. Such should especially

be the case for the diffusion characteristics of the faster atoms. (For easy reference, henceforth this theory will be referred to as TK1.)

Another treatment, based on an extension of the TKE, but motivated from the opposite end of the concentration scale (namely, the small particle concentration $c \rightarrow 0$), also suffers from similar problems.⁶ This theory (to be called TK2) is based on an equations-of-motion treatment whose truncations become increasingly inaccurate outside the range

$$zJ^0 < J^{\text{min}}, \quad (2.8)$$

where J^{min} is the smallest hopping rate. For most physical systems that one ordinarily deals with, the specified range of hopping rates may be wide enough to be useful. However, for situations where the hopping rates of the various components are vastly different, the TK2 cannot be expected to be satisfactory.

While the reader is best referred to the original⁶ for details, it is convenient to give below the final results obtained in TK2. The tracer diffusion correlation factor f^0 in a mixed *A-B* system is given as follows:

$$f^0 = [1 + 2J^0 \rho_0 / (M v_0)]^{-1}, \quad (2.9a)$$

where M is as defined in (2.3b) and

$$\rho_0 = vJ^0(c^A + c^B)J^B + c^B(1 - c^B)J^A - c^A c^B (J^A + J^B), \quad (2.9b)$$

$$v_0 = [vJ^0 + (1 - c^B)J^A][vJ^0 + (1 - c^A)J^B] - c^A c^B J^A J^B. \quad (2.9c)$$

III. SIMULATIONS AND ANALYSIS OF DATA IN TWO DIMENSIONS

A. Simulation procedure

The simulation routine for calculating tracer diffusion in a two-dimensional *A-B* alloy is carried out by a simple generalization of the routine given for the one-dimensional system (see the succeeding paper,¹⁰ henceforth to be referred as III). This generalization parallels closely that which is implicit in going from the one-dimensional one-component system¹¹ to the two-dimensional one-component system (see I). Consequently, to save space we shall not describe this routine in these pages.

In the two-dimensional square lattice, $z = 4$. Accordingly, in the following our attention will be focused on those relative sizes of the hopping rates J^B and J^A where the slower one lies between 100% to 10% of the faster one. In other words, the lowest value of the ratio η that we shall analyze is $\frac{1}{10}$. Clearly, such an η is just below the $1/z$ limit which, as mentioned earlier, is the natural lower limit of the theories described in Sec. II.

Two different types of samples were used. These comprised 100×100 and 150×150 site networks and were used when $c > \frac{1}{2}$. For $c \leq \frac{1}{2}$, larger networks, namely,

TABLE I. The diffusion correlation factors f^A and f^B of the A atoms (fast particles) and the B atoms (slow particles) are listed for a two-dimensional square lattice. Here $J^B/J^A = \eta = 0.5$. The first column represents the concentration of A atoms, c^A , and the second column gives c^B . The third column shows our numerical results obtained by simulating grand samples, each consisting of an effective number $N_G = 10^6$ particles. The fourth and fifth columns display the theoretical values of f^A predicted by theories TK2 and TK1, respectively. The last three columns follow the same sequence but refer instead to f^B .

| c^A | c^B | f^A | | | f^B | | |
|-------|-------|--------------------|------------|------------|--------------------|------------|------------|
| | | Simulation results | Theory TK2 | Theory TK1 | Simulation results | Theory TK2 | Theory TK1 |
| 0.60 | 0.2 | 0.512±0.002 | 0.5099 | 0.5339 | 0.664±0.003 | 0.6671 | 0.6715 |
| 0.15 | 0.15 | 0.788±0.005 | 0.7906 | 0.8051 | 0.850±0.008 | 0.8587 | 0.8598 |
| 0.10 | 0.20 | 0.784±0.005 | 0.7783 | 0.7960 | 0.847±0.008 | 0.8478 | 0.8506 |
| 0.40 | 0.40 | 0.471±0.002 | 0.4692 | 0.5003 | 0.620±0.003 | 0.6297 | 0.6366 |
| 0.20 | 0.60 | 0.427±0.002 | 0.4279 | 0.4669 | 0.585±0.002 | 0.5897 | 0.6021 |
| 0.20 | 0.10 | 0.803±0.005 | 0.8018 | 0.8141 | 0.866±0.008 | 0.8682 | 0.8689 |
| 0.25 | 0.25 | 0.655±0.003 | 0.6487 | 0.6802 | 0.752±0.006 | 0.7633 | 0.7689 |

150×150 and 200×200 sites were utilized. As in Ref. 1, the overall differences between the results provided by grand samples (GS's) of $N_G \geq 10^6$ particles each (obtained from the two different types of networks) were generally similar to the fluctuations within each of these grand samples.

To obtain reasonable long-time statistics, these simulations were run for $\tau = 2500$ Monte Carlo steps per particle (MCS/p) each. Generally speaking, for $\eta = \frac{1}{2}$, the long-time behavior had adequately set in for times $\tau \sim 250$ MCS/p. For $\eta = \frac{1}{10}$, however, the earliest time for which this behavior was assumed to be in place was 500 MCS/p.

B. Analysis

The analysis of the two-dimensional A - B alloy followed the pattern already set for the corresponding one-component system studied in I. The only difference between I and the present work is that here we have two separate sets of data: one relating to the mean-square displacement of the A atoms, i.e., $\langle \Delta X_A^2 \rangle_{(t)}$, and the other to that of the B atoms, i.e., $\langle \Delta X_B^2 \rangle_{(t)}$. As a consequence, we analyze these cases separately, albeit identically, to the one-component case described in I. This process yields two separate diffusion correlation factors, namely, f^A and f^B . These correlation factors are dependent, however, not only on the two concentrations c^A and c^B , they are also functions of the hopping rates ratio η .

IV. RESULTS IN TWO DIMENSIONS

Several large GS simulations on effective sample sizes of $N_G > 1$ million particles each were used to obtain estimates for the diffusion correlation factors f^A and f^B in an isotropic square lattice with $\eta = 0.5$ and 0.1. (Compare also the results for $\eta = 1$ given in paper I.) These estimates are expected to be accurate to within 2–5 parts per thousand. (See Tables I and II.)

In addition to the large-sample precision results, we also report several mini-grand-sample runs which averaged over only 70 000 particles each. These results (displayed as crosses in Figs. 1–3) incur much larger errors—between 1% and 10%—but in view of the ease of

the execution of these runs, they are found to be a useful supplement to the precision results (given in Tables I and II and shown in solid circles in Figs. 1–3) which were obtained from costly and time-consuming runs.

V. SIMULATIONS AND ANALYSIS OF DATA IN THREE DIMENSIONS

A. Simulation procedure

Monte Carlo simulations in three-dimensional minimally interacting systems have been described by many authors.^{10–15} The new feature of problem being discussed

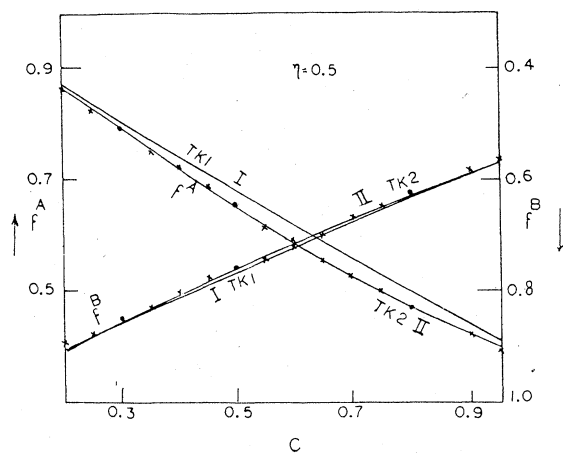


FIG. 1. Correlation factors f^A and f^B for the fast and the slow particles in two-dimensional quadratic lattices are plotted for $\eta = 0.5$ as a function of the total concentration of A and B atoms, i.e., $c = c^A + c^B = 2c^A$. The solid curves represent the theoretical results of theories TK1 and TK2 (indicated by indices I and II, respectively). The scale on the right refers to f^B and the one on the left corresponds to f^A . The solid circles represent the precision simulation results given in Table I. Similarly, the crosses indicate the simulation estimates obtained from the smaller, 70 000-particle samples.

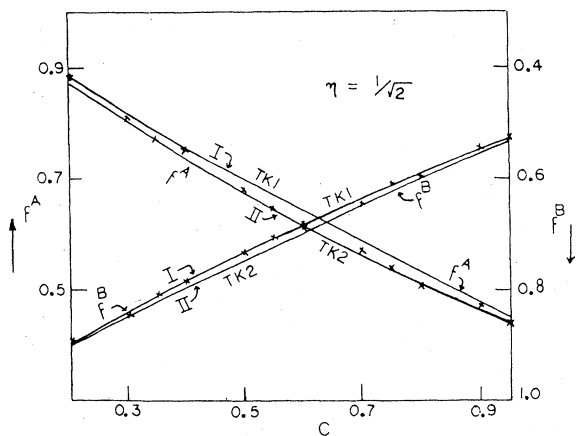


FIG. 2. Same as Fig. 1, except for η , which is $(\frac{1}{2})^{1/2}$.

here is that systems with macroscopic concentrations of two different varieties of atoms are being treated (compare also Ref. 12). However, this feature is readily incorporated into the simulation routine. (See the succeeding paper III for details.)

Simulations were run for up to 500 MCS/p for $\eta = (\frac{1}{2})^{1/2}$ and $c^A = c^B = c > \frac{1}{2}$. For $\eta = \frac{1}{3}$ and $c > \frac{1}{2}$, they were run for 660 MCS/p. For $c < \frac{1}{2}$, or $\eta = \frac{1}{10}$, the runs were carried through to 1000 MCS/p while for $c < \frac{1}{2}$ and $\eta = \frac{1}{10}$ the time limit was set at 2500 MCS/p. As before, two different sets of network sizes were utilized. When the maximum MCS/p used was 660 or less, simple-cubic networks of $20 \times 20 \times 20$ and $26 \times 26 \times 26$ sites each were used. For systems where the maximum time span was 1000 MCS/p, or longer, the networks were larger, i.e., $26 \times 26 \times 26$ and $30 \times 30 \times 30$.

As in two dimensions, both large effective systems (GS sizes of $N_G \geq 10^6$ atoms each) and small systems (mini-GS sizes of $N_G \sim 70\,000$ particles each) were used. The accu-

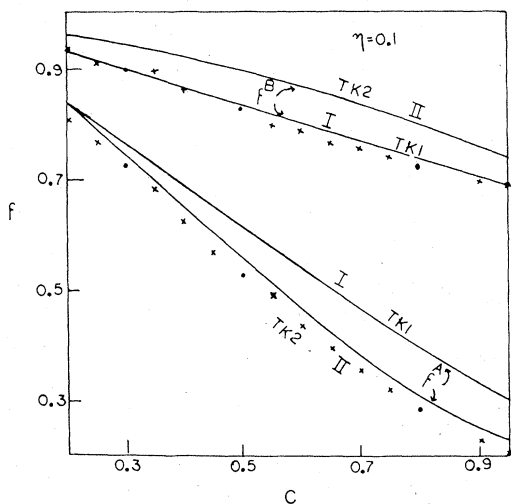


FIG. 3. Similar to Fig. 1, with the following changes: Here $\eta = 0.1$, and the left-hand scale refers to both f^A and f^B .

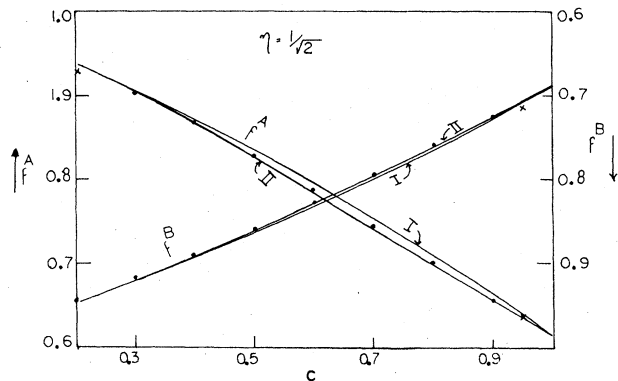


FIG. 4. Similar to Fig. 1 with two differences. First, this figure refers to a three-dimensional simple-cubic lattice. Second, here the ratio is $\eta = (\frac{1}{2})^{1/2}$.

racy obtainable from the smaller systems is approximately 3–5 times worse. However, because the computer time used in the simulations is proportional to the overall system size, the mini-GS's were proportionately 15 times less costly to simulate. Their results are, nevertheless, only of qualitative value.

B. Analysis

Monte Carlo simulations in three-dimensional systems^{10–15} have usually relied on achieving the “long-time” limit. Therefore, the Einstein proportionality formula, relating the mean-square displacement along a given axis to the diffusion coefficient D and the time elapsed τ , is used.

In practice, however, the relevant (MCS/p) time τ cannot be inordinately long. As a result, the standard Einstein formula needs to be supplemented with additional terms, i.e.,

$$\Delta_\lambda(\tau) = 2J^\lambda f^\lambda v\tau + \text{const} + O(J^\lambda \tau)^{-1/2}. \quad (5.1)$$

Here, $\Delta_\lambda(\tau)$ is the mean-square displacement after time τ of a particle of variety λ measured along one of the three

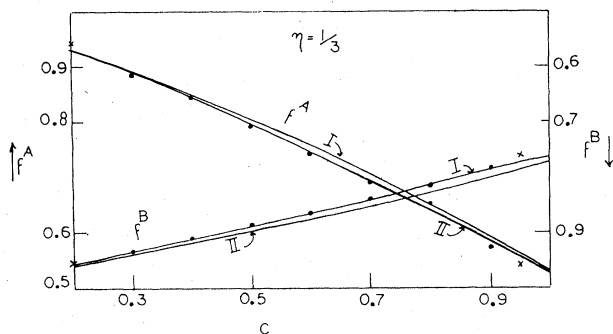


FIG. 5. Same as Fig. 4, with the difference that here $\eta = \frac{1}{3}$.

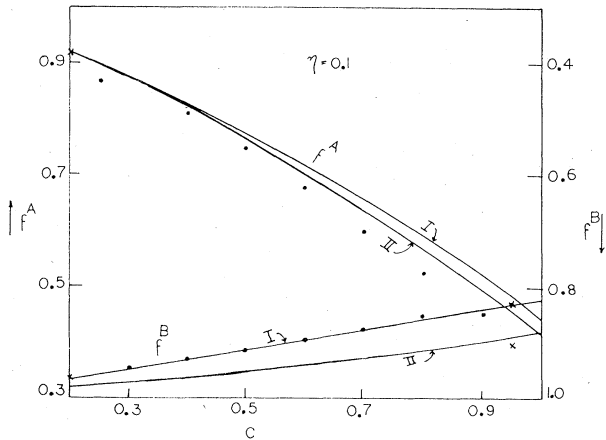


FIG. 6. Same as Fig. 4, except that now $\eta = \frac{1}{10}$.

Cartesian axes (for best statistics, Δ_λ is computed along all three axes and an average is then taken). The corresponding hopping rate (assumed to be spatially isotropic) is J^λ , v is the vacancy concentration and f^λ is the diffusion correlation factor of interest. Clearly, the unknown constant appearing in Eq. (5.1) is in itself of no particular importance. On the other hand, its absolute size is usually of order 0.1–1, and thus its neglect can cause errors of order 1% or so when the longest times used are of order 100–500. Accordingly, it is unwise to ignore the constant in Eq. (5.1).

Therefore, in analogy with the description given in I, we proceed as follows: Choose an initial time τ_0 , which is long enough for the long-time behavior to have set in. (More will be said regarding this point later.) For a time $\tau_1 > \tau_0$, write

$$\begin{aligned} L_\lambda(\tau_1, \tau_0) &= \Delta_\lambda(\tau_1) - \Delta_\lambda(\tau_0) \\ &= 2J^\lambda f^\lambda v (\tau_1 - \tau_0) \\ &\quad + O[(1/J^\lambda)(1/\tau_1)^{1/2} - (1/\tau_0)^{1/2}]. \end{aligned}$$

Then look for the slope S_λ from the relationship

$$S_\lambda(\tau_1, \tau_0) = L_\lambda(\tau_1 - \tau_0) / (\tau_1 - \tau_0) + R. \quad (5.2)$$

It is clear that the remainder R on the right-hand side of Eq. (5.2) is of order $(\tau_0 \tau_1)^{-1/2}$. For large enough τ_0 and τ_1 , this is obviously much smaller than the constant occurring in Eq. (5.1) and can therefore more safely be ignored.

Because S_λ is in general a function of both τ_0 and τ_1 , it is best to take an average over the ensemble of such slopes that are obtained for all τ_0 and τ_1 so that the maximum value of τ_1 is at least 200 MCS/ p smaller than the maximum length of the run. (This is to make sure that the last interval over which the slope is measured is at least 200 MCS/ p wide.) Both the average \bar{S}_λ and its root-mean-square deviation δS_λ are recorded. The diffusion correlation factor f^λ is now readily obtained from the relation

$$f_\lambda = \bar{S}_\lambda / (2J^\lambda v). \quad (5.3)$$

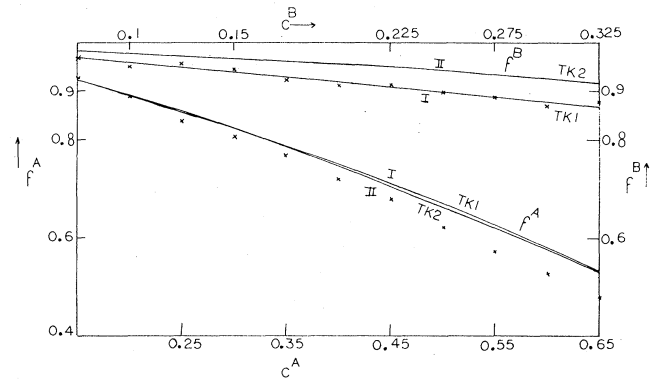


FIG. 7. Simple-cubic lattice correlation factors f^A and f^B are plotted as functions of c^A (or c^B). Here $\eta = 0.1$ and $c^A = 2c^B$. The solid curves represent the theoretical results of TK1 (shown as I) and TK2 (shown as II). The crosses indicate small-sample simulation results utilizing 70 000 particles.

The quantity $\delta S_\lambda / (2J^\lambda v) \equiv \delta_\lambda$ provides a workable measure of the inaccuracy to be expected. It is interesting that generally speaking δ_λ is also similar to the magnitude of the discrepancy between the two f_λ 's computed from the "large" and the "small" network sizes mentioned earlier. Therefore, in what follows, we shall refer to δ_λ as being a meaningful estimate of the error in f_λ .

VI. RESULTS IN THREE DIMENSIONS

For a three-dimensional, simple-cubic lattice, diffusion correlation factors f^A and f^B for a binary A - B alloy with $\eta = (\frac{1}{2})^{1/2}$, $\frac{1}{3}$, and $\frac{1}{10}$ are listed in Tables III, IV, and V, respectively. These precision results were obtained from large GS's with $N_G > 10^6$ particles each. For ready reference, the corresponding predictions of both the theories TK1 and TK2 are also included. These simulations are expected to be accurate to within 2–6 parts per thousand. To aid the perusal of the tables, most of these results are also displayed in the form of figures, Figs. 4–8.

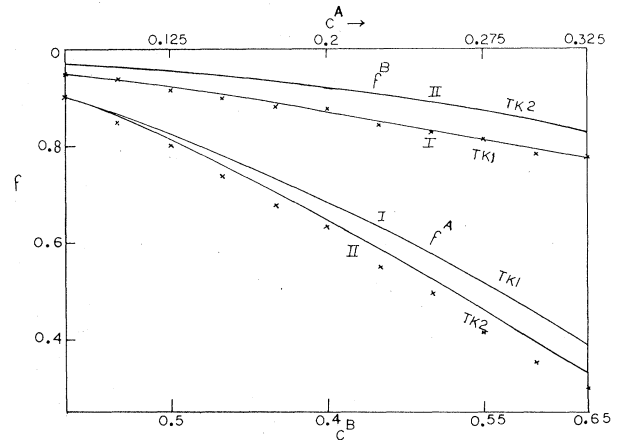


FIG. 8. Similar to Fig. 7, with the difference that here $c^B = 2c^A$.

TABLE II. Similar to Table I, but here the ratio is $\eta=0.1$.

| c^A | c^B | Simulation results | f^A | | Simulation results | f^B | |
|---------------|---------------|--------------------|------------|------------|--------------------|------------|------------|
| | | | Theory TK2 | Theory TK1 | | Theory TK2 | Theory TK1 |
| 0.2 | 0.6 | 0.186±0.002 | 0.1910 | 0.3249 | 0.635±0.003 | 0.6765 | 0.6524 |
| 0.4 | 0.4 | 0.284±0.002 | 0.3124 | 0.4041 | 0.722±0.003 | 0.8014 | 0.7389 |
| $\frac{1}{3}$ | $\frac{1}{6}$ | 0.589±0.003 | 0.6184 | 0.6524 | 0.867±0.005 | 0.9206 | 0.8723 |
| 0.1 | 0.2 | 0.693±0.007 | 0.7127 | 0.7438 | 0.876±0.008 | 0.9238 | 0.8774 |
| 0.25 | 0.25 | 0.528±0.004 | 0.5599 | 0.6169 | 0.826±0.005 | 0.8958 | 0.8348 |
| 0.6 | 0.2 | 0.415±0.002 | 0.4448 | 0.4851 | 0.820±0.004 | 0.8749 | 0.8274 |
| $\frac{1}{6}$ | $\frac{1}{3}$ | 0.455±0.005 | 0.4876 | 0.5818 | 0.787±0.005 | 0.8571 | 0.7977 |
| 0.15 | 0.15 | 0.727±0.007 | 0.7492 | 0.7957 | 0.897±0.008 | 0.9428 | 0.9001 |

TABLE III. Diffusion correlation factors f^A and f^B are listed for a three-dimensional, simple-cubic lattice for the case $c^A=c^B$ and $\eta=(\frac{1}{2})^{1/2}$. Excepting the two samples marked with asterisks (see the first column), these are the precision simulation results obtained from large GS's with effective particle numbers $N_G \geq 10^6$ each. The two values with asterisks are less accurate mini-GS's with 70 000 particles each.

| c^A | Precision simulation | f^A | | Precision simulation | f^B | |
|--------|----------------------|--------|--------|----------------------|--------|--------|
| | | TK2 | TK1 | | TK2 | TK1 |
| 0.475* | 0.637*±0.010 | 0.6348 | 0.6387 | 0.716*±0.015 | 0.7093 | 0.7104 |
| 0.450 | 0.655 ±0.003 | 0.6560 | 0.6634 | 0.727 ±0.003 | 0.7264 | 0.7293 |
| 0.400 | 0.700 ±0.003 | 0.6991 | 0.7103 | 0.758 ±0.003 | 0.7607 | 0.7656 |
| 0.350 | 0.745 ±0.003 | 0.7424 | 0.7544 | 0.796 ±0.003 | 0.7946 | 0.8001 |
| 0.300 | 0.789 ±0.004 | 0.7850 | 0.7958 | 0.827 ±0.003 | 0.8279 | 0.8328 |
| 0.250 | 0.828 ±0.004 | 0.8264 | 0.8348 | 0.860 ±0.003 | 0.8601 | 0.8640 |
| 0.200 | 0.868 ±0.004 | 0.8658 | 0.8716 | 0.891 ±0.005 | 0.8911 | 0.8938 |
| 0.150 | 0.904 ±0.006 | 0.9031 | 0.9063 | 0.919 ±0.007 | 0.9207 | 0.9222 |
| 0.100* | 0.929*±0.015 | 0.9379 | 0.9392 | 0.946*±0.015 | 0.9487 | 0.9493 |

TABLE IV. Similar to Table III, except that here $\eta=\frac{1}{3}$.

| c^A | Precision simulation | f^A | | Precision simulation | f^B | |
|--------|----------------------|--------|--------|----------------------|--------|--------|
| | | TK2 | TK1 | | TK2 | TK1 |
| 0.475* | 0.540*±0.0100 | 0.5583 | 0.5630 | 0.760*±0.015 | 0.7874 | 0.7728 |
| 0.450 | 0.571 ±0.0025 | 0.5847 | 0.5942 | 0.782 ±0.004 | 0.8010 | 0.7870 |
| 0.400 | 0.625 ±0.0025 | 0.6388 | 0.6531 | 0.807 ±0.004 | 0.8274 | 0.8146 |
| 0.350 | 0.688 ±0.003 | 0.6933 | 0.7077 | 0.839 ±0.004 | 0.8527 | 0.8410 |
| 0.300 | 0.741 ±0.003 | 0.7465 | 0.7583 | 0.865 ±0.004 | 0.8769 | 0.8664 |
| 0.250 | 0.791 ±0.004 | 0.7974 | 0.8055 | 0.888 ±0.004 | 0.9000 | 0.8908 |
| 0.200 | 0.843 ±0.004 | 0.8451 | 0.8496 | 0.911 ±0.004 | 0.9219 | 0.9143 |
| 0.150 | 0.886 ±0.005 | 0.8892 | 0.8908 | 0.936 ±0.005 | 0.9429 | 0.9369 |
| 0.100* | 0.945*±0.015 | 0.9297 | 0.9295 | 0.959*±0.015 | 0.9628 | 0.9587 |

TABLE V. Similar to Table III, except that here $\eta = \frac{1}{10}$.

| c^A | f^A | | | f^B | | |
|--------|----------------------|--------|--------|----------------------|--------|--------|
| | Precision simulation | TK2 | TK1 | Precision simulation | TK2 | TK1 |
| 0.475* | 0.400*±0.010 | 0.4598 | 0.4819 | 0.830*±0.015 | 0.8906 | 0.8233 |
| 0.450 | 0.453 ±0.002 | 0.4953 | 0.5207 | 0.859 ±0.004 | 0.8996 | 0.8386 |
| 0.400 | 0.522 ±0.002 | 0.5677 | 0.5931 | 0.851 ±0.004 | 0.9159 | 0.8588 |
| 0.350 | 0.598 ±0.002 | 0.6391 | 0.6593 | 0.874 ±0.004 | 0.9301 | 0.8784 |
| 0.300 | 0.675 ±0.002 | 0.7069 | 0.7200 | 0.895 ±0.004 | 0.9426 | 0.8973 |
| 0.250 | 0.746 ±0.0025 | 0.7695 | 0.7759 | 0.915 ±0.004 | 0.9539 | 0.9157 |
| 0.200 | 0.807 ±0.003 | 0.8264 | 0.8275 | 0.931 ±0.005 | 0.9643 | 0.9335 |
| 0.150 | 0.865 ±0.003 | 0.8774 | 0.8754 | 0.950 ±0.005 | 0.9739 | 0.9509 |
| 0.100* | 0.920*±0.01 | 0.9231 | 0.9199 | 0.966*±0.015 | 0.9830 | 0.9677 |

TABLE VI. Small sample ($N_G \sim 70\,000$ particles each) simulation results for diffusion correlation factors f^A and f^B in a simple-cubic system with $\eta = \frac{1}{10}$, with $c^A = 2c^B$.

| c^A | f^A | | | f^B | | |
|-------|-------------------------|--------|--------|-------------------------|--------|--------|
| | Small-sample simulation | TK2 | TK1 | Small-sample simulation | TK2 | TK1 |
| 0.650 | 0.462±0.015 | 0.5359 | 0.5353 | 0.878±0.035 | 0.9180 | 0.8687 |
| 0.550 | 0.568±0.012 | 0.6226 | 0.6301 | 0.875±0.03 | 0.9350 | 0.8908 |
| 0.500 | 0.617±0.015 | 0.6658 | 0.6734 | 0.881±0.025 | 0.9423 | 0.9016 |
| 0.450 | 0.685±0.015 | 0.7079 | 0.7143 | 0.902±0.02 | 0.9492 | 0.9122 |
| 0.400 | 0.723±0.015 | 0.7486 | 0.7530 | 0.874±0.02 | 0.9557 | 0.9226 |
| 0.350 | 0.777±0.020 | 0.7874 | 0.7896 | 0.904±0.025 | 0.9619 | 0.9329 |
| 0.300 | 0.813±0.020 | 0.8242 | 0.8243 | 0.951±0.030 | 0.9679 | 0.9429 |
| 0.250 | 0.854±0.030 | 0.8588 | 0.8573 | 0.952±0.035 | 0.9736 | 0.9529 |
| 0.200 | 0.893±0.030 | 0.8912 | 0.8886 | 0.970±0.05 | 0.9792 | 0.9626 |
| 0.150 | 0.925±0.030 | 0.9214 | 0.9185 | 0.961±0.07 | 0.9846 | 0.9722 |

TABLE VII. Same as Table VI, except that here $2c^A = c^B$.

| c^A | f^A | | | f^B | | |
|-------|-------------------------|--------|--------|-------------------------|--------|--------|
| | Small-sample simulation | TK2 | TK1 | Small-sample simulation | TK2 | TK1 |
| 0.650 | 0.281±0.020 | 0.3332 | 0.3813 | 0.796±0.035 | 0.8298 | 0.7741 |
| 0.600 | 0.338±0.015 | 0.3911 | 0.4519 | 0.788±0.030 | 0.8526 | 0.7947 |
| 0.550 | 0.415±0.012 | 0.4548 | 0.5170 | 0.815±0.025 | 0.8730 | 0.8146 |
| 0.500 | 0.493±0.012 | 0.5215 | 0.5773 | 0.817±0.020 | 0.8911 | 0.8339 |
| 0.450 | 0.538±0.015 | 0.5878 | 0.6333 | 0.846±0.020 | 0.9070 | 0.8527 |
| 0.400 | 0.621±0.015 | 0.6515 | 0.6853 | 0.876±0.025 | 0.9211 | 0.8709 |
| 0.350 | 0.661±0.02 | 0.7110 | 0.7339 | 0.867±0.020 | 0.9337 | 0.8886 |
| 0.300 | 0.712±0.02 | 0.7656 | 0.7793 | 0.876±0.025 | 0.9451 | 0.9059 |
| 0.250 | 0.799±0.02 | 0.8152 | 0.8219 | 0.905±0.025 | 0.9556 | 0.9226 |
| 0.200 | 0.839±0.03 | 0.8601 | 0.8619 | 0.938±0.035 | 0.9654 | 0.9389 |
| 0.150 | 0.928±0.04 | 0.9006 | 0.8995 | 0.945±0.035 | 0.9747 | 0.9548 |

VII. DISCUSSION AND CONCLUDING REMARKS

It is clear from Tables I–VII that for the larger ratios η , i.e., for $\eta \geq \frac{1}{2}$, both the theories TK1 and TK2 are adequate. In particular, TK2 works well over the entire range of concentrations and its accuracy is roughly comparable to that of the simulation “experiment” itself.

The self-consistent theory TK1, on the other hand, works satisfactorily only for the diffusion correlation factor relating to the slow atoms (which means, in the present case, f^B). This feature of the theory though is not entirely unexpected. What is quite surprising, however, is the degree to which the TK1 predictions for f^A (namely, the correlation factor for the fast atoms) are in error. It is observed that even for $\eta = \frac{1}{3}$, which is well within the range (2.6), the TK1 estimates for f^A are in error by 2–5% over a wide range of concentration. (They are systematically *too high*. See Figs. 1–8.)

For $\eta = \frac{1}{10}$, we are already outside the range where these theories are expected to be adequate. A perusal of Tables II and V–VII and a look at Figs. 3 and 6–8 confirm this expectation: for $\eta = \frac{1}{10}$, even TK2 is seen to be in error by approximately 3–10%. Qualitatively speaking, however, the predictions of TK2 are not unreasonable. Nevertheless, it is abundantly clear that the inequality (2.8) does indeed provide a realistic definition of the allowed range of hopping rates outside which the present theories have marginal applicability.

An interesting and unanticipated observation that emerges from these simulations is a new type of complementarity between the theories TK1 and TK2. What we mean here is that while on general grounds a certain complementarity between the two theories was indeed ex-

pected, it referred only to the concentration ranges, namely, that TK1 is a theory derived from the $v \rightarrow 0$ limit, whereas TK2 is an outgrowth of the $c \ll 1$ decouplings. What has emerged, however, is different. TK2 is found to be better overall, including the intermediate concentration regime, but it is especially so for the diffusion characteristics of the fast atoms, i.e., for f^A . On the other hand, TK1, despite its intrinsic self-consistency, is inferior overall. Nevertheless, TK1 does moderately well for the *slow* atoms. With this empirical observation in hand, one can perhaps use TK1 and TK2 in combination to make predictions outside the range specified by the inequality (2.8).

To sum up, the existing theories for the labeled particle diffusion in the mixed, random dynamic alloys in two and three dimensions are qualitatively useful within the range specified by the inequalities (2.6) and (2.8). Outside this range, the theories can only be used as empirical aids in interpreting the data. When this is done, TK1 should be used for the *slow* atoms and TK2 for the *fast* ones.

Note added in proof. A proper self-consistent theory has now been worked out [see R. A. Tahir-Kheli, *Philos. Mag.* (to be published)] which satisfactorily explains all the Monte Carlo data [also see P. Holdsworth and R. J. Elliott, *Philos. Mag.* (to be published)].

ACKNOWLEDGMENTS

This work was supported by the National Science Foundation. We are greatly indebted to R. J. Elliott, J. D. Gunton, R. B. Stinchcombe, P. Beal, P. Leath, and P. Holdsworth for helpful discussions.

- ¹R. A. Tahir-Kheli and Nagwa EL-Meshad, preceding paper, *Phys. Rev. B* **32**, 6166 (1985).
- ²J. R. Manning, *Phys. Rev. B* **4**, 1111 (1971).
- ³For a review of the earlier work, see J. R. Manning, *Diffusion Kinetics for Atoms in Crystals* (Van Nostrand, Princeton, N.J., 1968).
- ⁴H. J. DeBruin, G. E. Murch, H. Bakker, and L. P. van der Mey, *Thin Solid Films* **25**, 47 (1975).
- ⁵R. A. Tahir-Kheli, *Phys. Rev. B* **28**, 3049 (1983).
- ⁶R. A. Tahir-Kheli, *Phys. Rev. B* **28**, 2257 (1983).
- ⁷R. A. Kikuchi and H. Sato, *J. Chem. Phys.* **53**, 2702 (1970).
- ⁸H. J. DeBruin, H. Bakker, and L. P. van der May, *Phys. Status Solidi B* **82**, 581 (1977).
- ⁹R. A. Tahir-Kheli and R. J. Elliott, *Phys. Rev. B* **27**, 844

- (1983).
- ¹⁰R. A. Tahir-Kheli and Nagwa El-Meshad, following paper, *Phys. Rev. B* **32**, 6184 (1985).
- ¹¹For recent reviews, see G. E. Murch, in *Diffusion in Crystalline Solids*, edited by G. E. Murch and A. S. Nowick (Academic, New York, 1984); also, K. W. Kehr and K. Binder (unpublished).
- ¹²R. Kutner and K. W. Kehr (unpublished).
- ¹³G. E. Murch and S. J. Rothman, *Philos. Mag. A* **43**, 229 (1981).
- ¹⁴G. E. Murch, *Philos. Mag. A* **49**, 21 (1984).
- ¹⁵R. Kutner, K. Binder, and K. W. Kehr, *Phys. Rev. B* **26**, 2467 (1982).